Preliminary Results of Large Supersonic Burning Combustor Testing

A. J. Metzler* and T. W. Mertz†
NASA Lewis Research Center,
Cleveland, Ohio

A hydrogen fueled supersonic-burning combustor 18 in. in diameter, which is equivalent to that of an engine about 6 ft in diameter, was tested as a direct-connected duct at inlet conditions which simulated Mach 8 flight at 115,000 ft alt. A synthetic air consisting of oxygen with 39% nitrogen and 38% water vapor at a total temperature of 4500°R and a total pressure of 300 psia was supplied to the combustor inlet by a hydrazine-nitrogen tetroxide hot gas generator which maintained a uniform inlet flow Mach number of 2.8. The large combustor size required a new approach to fuel injector design. Some hydrogen was injected through flush-wall injectors, but most was injected from two rows of swept and tapered struts immersed in the flow stream. Supersonic combustion was obtained at hydrogen equivalence ratios of 0.94 without encountering thermal choking. Wall static pressures, and the radial distribution of hydrogen, Pitot pressure, and Mach number were determined at the combustor exit.

Introduction

SUPERSONIC burning combustors proposed for hypersonic airbreathing vehicles would operate at such high levels of stagnation pressure, temperature, and mass flow rates that it will be extremely difficult to reproduce combustor inlet conditions in ground test facilities. Therefore, testing of such advanced concept combustors has generally been limited and subject to compromise. In order to ease test facility air supply requirements, testing has been largely restricted to short duration testing or to combustors of very small cross section which have usually employed flush-wall injection schemes for the hydrogen fuel. This type of fuel injection appears to be inadequate for good fuel distribution in large combustors because of the low-penetration distances attainable with hydrogen jets into supersonic air streams.[1] Strut type injectors may be required to optimize fuel distribution in combustors with large cross sectional areas. Such combustors would be expected to have injection-mixing-combustion interactions appreciably different from those occurring in wall-injection combustors. Therefore small scale combustor testing may adequately predict parametric trends but performance data cannot be scaled to such large size combustors. Furthermore the problems of strut blockage, drag, and heat transfer, as they affect the over-all combustor design and performance, can only be evaluated by tests of larger scale combustor hardware. Although supersonic burning in small ducts has been demonstrated, the practicality of the concept of a supersonic burning combustor of more complex design for large scale hardware has not been previously demonstrated.

The purpose of the large scale combustor test program reported herein was two-fold. The use of a hot gas generator[2] for large scale supersonic combustor testing was to be demonstrated. Secondly, supersonic combustion was to be demonstrated in large scale hardware of a practical geometry, at a single set of combustor inlet conditions, in order to obtain preliminary test information pertinent to injector-combustor design, operation, and performance. Since combustor studies of this type were without precedent, it was also intended to define some of the problem areas for future, more detailed studies.

Combustor inlet conditions of pressure, temperature, and Mach number were estimated for a hypothetical vehicle flight at Mach 8. A simulated flight altitude of 115,000 ft (35 km) is estimated from the facility stagnation pressure limitation of 300 psia (2.06×10^6 N/m^2) and an assumed inlet contraction ratio and total pressure recovery. Air composition was not duplicated. Ideally, inlet gases contained approximately 21 Vol. % oxygen with the remainder nearly equal molar concentrations of nitrogen and water vapor plus a residual concentration of free radicals produced in the gas generator and kinetically frozen during the nozzle expansion. However, as a result of chemical inefficiency and the nozzle expansion process, an appreciable concentration of NO was probably also present. The net effect of the water vapor and radical concentrations on the combustor performance is not known, but it is believed to be relatively unimportant.[3] Stream static temperature was near 1200°K, and the temperatures in the ignition regions were expected to be appreciably higher as a result of shock interactions. As a result, the net effect of vitiation on the ignition delay is expected to be minor, and was second order to the purpose of the experimental tests. Also, recombination kinetics which may influence the exothermic radical recombination reactions are only affected by the water as a third body, so that these reaction rates would then be proportional to the concentration of the water in the reacting gases. Since appreciable concentrations of water are normally present in the combustor as a result of bimolecular radical reactions, the additional water in the vitiated stream should have only second-order effects. For the conditions of these tests, heat release rates are believed to be mixing limited rather than limited by reaction kinetics.

A supersonic burning combustor was tested as a direct-connected duct using a hydrazine-nitrogen tetroxide rocket as the combustor inlet-gas generator. All hardware was water cooled. The combustor had an inlet i.d. of 18 in. (45.7 cm) which might be equivalent to the combustor size for an engine about 2 m in diameter. The combustor was fueled with gaseous hydrogen at ambient temperature.

This paper reports the results of combustor tests at a single set of inlet flow conditions for a range of hydrogen equivalence ratios from 0–0.94. For most tests, burn time was 15 sec, and all data were taken during steady-state conditions. The test results reported are preliminary and do not include measurements of combustor thrust or combustion efficiency. Only

Received July 30, 1970; revision received September 1, 1971.
Index category: Hypersonic Airbreathing Propulsion.

* Aerospace Research Scientist, Hypersonic Propulsion Section. Member AIAA.
† Aerospace Research Scientist, Hypersonic Propulsion Section. Associate Member AIAA.

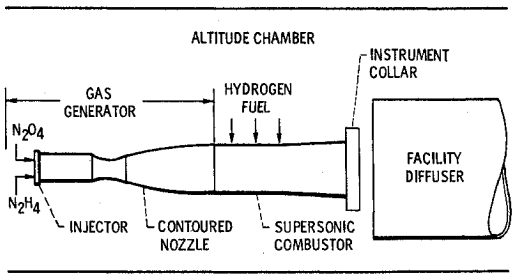

Fig. 1 Schematic of combustor test facility.

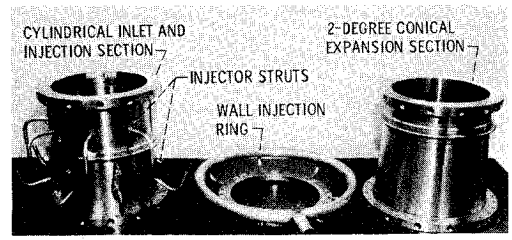

Fig. 2 Disassembled combustor test hardware.

a single basic hydrogen injector geometry having a maximum transverse duct blockage of 4.75% was tested. The effects of blockage and injector drag were not measured. Nevertheless these tests did indicate that strut-type fuel injectors could be maintained in the severe environments anticipated for advanced airbreathing engines if separate cooling circuits are provided for high-heat flux leading edge regions. This combustor test program was performed in an altitude test chamber at the Lewis Research Center, Cleveland, Ohio.

Facility and Test Hardware

The combustor test facility is shown schematically in Fig. 1 as it was installed in the altitude tank. The gas generator with contoured nozzle and test combustor were assembled as a direct-connect duct exhausting as a freejet into the altitude chamber which was pumped to about one-fifth atm. The combustor exhaust was collected by a diffuser prior to entering the vacuum piping. All hardware was water cooled.

Combustor test conditions were selected to match stagnation air temperature at a flight Mach number of 8. Inlet pressure was determined by the 300 psia (2.06×10^6 N/m^2) design limit of the gas generator, and the inlet Mach number of 2.8 resulted from a reasonable estimate of the inlet geometric contraction ratio. The combustor inlet total pressure of 300 psia would correspond to a flight altitude of 115,000 ft (35 Km) if an inlet total pressure recovery of 20% is assumed.

Gas Generator

The gas generator was a rocket combustor which burned the hypergolic propellants hydrazine-nitrogen tetroxide. The rocket injector was developed specifically for stable, high performance at 300 psia (2.06×10^6 N/m^2) chamber pressure at an oxidant-fuel ratio (O/F) equal to 3.0. Preliminary injector tests[2] had indicated problems with the development of a gas generator of this type since combustion was frequently unstable and could cause gas generator damage. A specific like-on-like parallel-fan injector design[4] demonstrated very stable performance at design conditions together with a high characteristic velocity (C^*) efficiency. C^* efficiency was 97–98% which is equivalent to a combustion efficiency of 94–96%. Stable runs of 20 sec duration were attained, and longer run time with no injector damage would have been possible.

The combustion chamber had an i.d. of 10.78 in. (27.4 cm) and a characteristic length (L^*) of 38 in. for a nominal chamber length of 20 in. (50.8 cm). The like-on-like parallel-fan design had 360 elements drilled into the injector face. At design conditions, propellant mass flow was 99 lb (44.9 kg) per sec. Run time for this phase of the program was restricted to 15 sec but was practically limited to 100 sec by the total oxidant storage capacity available. High-frequency response pressure instrumentation verified that stable combustion performance was obtained. No injector deterioration was noted after a total run time of 5 min which included 32 separate ignition sequences.

The inlet nozzle was contoured for parallel flow and Mach 2.8 at the 18 in (45.7-cm) diam exit. The nozzle contour was designed according to the real gas method of characteristics which used a starting line determined by Sauer's method.[5] The inviscid contour was corrected by the boundary layer displacement thickness calculated by the method of Reshotko and Tucker.[6] The contoured nozzle was a machined and welded aluminum forging. Instrumentation measured the flow rates, temperature, and pressures necessary to calculate gas generator performance, to monitor coolant system operation and measure heat loss, and to evaluate the nozzle exit flow.

Combustor Test Hardware

The combustor consisted of the hydrogen injector struts and three duct sections pictured in Fig. 2. The sequence of assembly is from left to right with the inlet to each section located at the top of the figure. The combustor consisted of a constant area inlet and injection section (left), a wall injection ring (center), and an expansion section (right). The injection and expansion sections were fabricated as double wall structures for water cooling; the injection ring was hydrogen cooled. Features of the assembly of the combustor are detailed in Fig. 3. The combustor inlet section was a nickel cylinder 18 in. (45.7 cm) i.d. by 25 in. (63.5 cm) long. Mounting plates for 16 hydrogen injection struts were equally spaced at two axial locations as shown in the figure. The wall-injection ring was 1.3 in. (3.3 cm) wide with an i.d. of 18.38 in. (46.7 cm) which matched that of the expansion section inlet. A circumferential step 0.188 in. (0.478 cm)

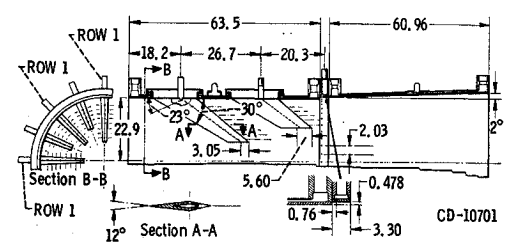

INJECTOR DRILLING LOCATIONS DISTANCE FROM WALL, CM
3.18
4.52
5.99
7.62
9.47
13.08
14.96
16.92

Fig. 3 Pertinent details of test combustor assembly.

high was thus formed with the cylindrical inlet section. In the wake of this step, hydrogen was injected through 72 equally-spaced holes 0.1695 in. (0.4305 cm) in diameter. The ring was cooled by the injected hydrogen flow. The inner shell of the conical expansion section of the combustor was mild steel flame-spray coated with zirconium oxide. The cone inlet i.d. was 18.38 in. (46.7 cm) with an expansion half-angle of 2°.

The hydrogen injector struts were designed to penetrate the inlet flow stream to distribute the hydrogen across the stream as uniformly as possible with minimum flow disturbance and blockage. The injectors were single nickel shells cooled by the injected hydrogen. The struts swept rearward at 30° (Fig. 3) and had a diamond shaped cross section aligned with the flow stream. Sonic flow injection orifices were drilled at the knee of the diamond and at the trailing edge. The injection orifices were 0.141 and 0.156 in. (0.358 and 0.396 cm) in diameter. The internal flow of the injected gaseous hydrogen cooled the struts. Initially the only provision that we made to adjust the coolant flow to the nonuniform heat flux was to deflect the incoming gas toward the leading edge of the injector. A simple plate inclined at 67° to the hydrogen flow direction at the injector inlet was used for this purpose. This cooling method proved inadequate and required subsequent modification. In the modified injector struts, the leading edge was cooled with a separate hydrogen coolant tube, 0.125-in. o.d. (0.317-cm) with a 0.020-in. (0.051-cm) wall, which formed the strut leading edge. The internal hydrogen flow adequately cooled the sides of the injector strut.

Four injector struts penetrated the stream 7 in. (17.8 cm) from the inner combustor wall, and four penetrated 6.25 in. (15.8 cm). These were located in the first row as shown in Fig. 3. Second row injectors all penetrated the stream 4.10 in. (10.4 cm).

Combustor Instrumentation

One injector in each row was specially instrumented to measure internal hydrogen pressure and pressure drop, surface temperatures, and surface static pressure. A Pitot tube was installed on the leading edge of one first row strut (Fig. 4).

Each combustor section had 0.026 in. (0.066 cm) diameter wall static pressure taps spaced along the length of the combustor at two circumferential positions. As shown in Fig. 5, one series of taps was in line with a first row injector strut and the other was midway between the first and second row strut positions. Wall thermocouples were similarly positioned, but in the cylindrical section only, to monitor gas-side and coolant-side wall temperatures. Figure 5 also shows the relative positioning of the pressure tap in the

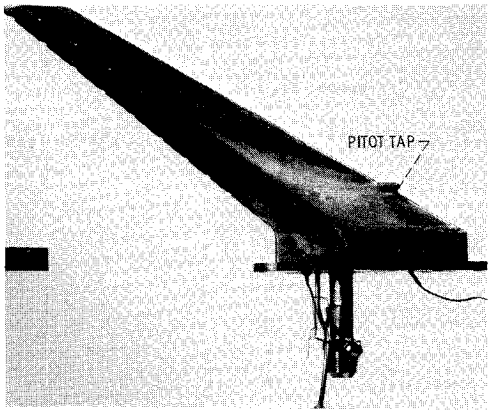

Fig. 4 Hydrogen injector strut.

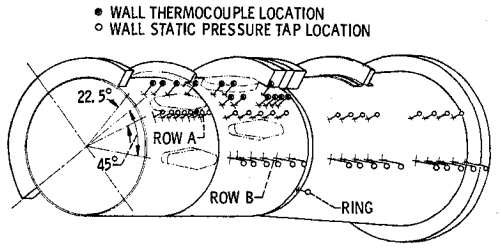

PRESSURE TAP LOCATIONS (CM)

ROW A			ROW B		RING
7.6	33.0	73.7	35.6	72.5	65.3
10.2	38.1	78.7	38.1	76.2	
12.7	43.2	83.8	40.6	81.3	
15.2	48.3	88.9	45.7	86.4	
17.8	53.3	104.1	50.8	91.4	
20.3		109.2	55.9	103.8	
22.9		114.3		106.7	
25.4		119.4		111.8	
				116.8	
				119.4	

Fig. 5 Orientation of hydrogen injectors and combustor wall instrumentation.

hydrogen injector ring. Fixed rake and traversing probe instrumentation was used to measure the radial distribution of gas stream total and static pressures at the combustor inlet and exit.

In addition a multipoint rake mounted across the gas stream at these locations was used to remove samples and measure Pitot pressure or to measure stream total temperature. The rake and a detail of one of the sample ports is shown in Fig. 6. The rake was developed for this program to measure the inlet-stream total temperature using a bare-wire radiation-cooled Iridium vs Iridium—40% Rhodium thermocouple. Thermocouple corrections for radiation ranged from 100°–185° R for the temperatures of interest for the assumption of radiation to walls at coolant temperature. The thermocouples were readily removable through the sample ports so the rake might also be used for gas sampling or Pitot pressure measurements.

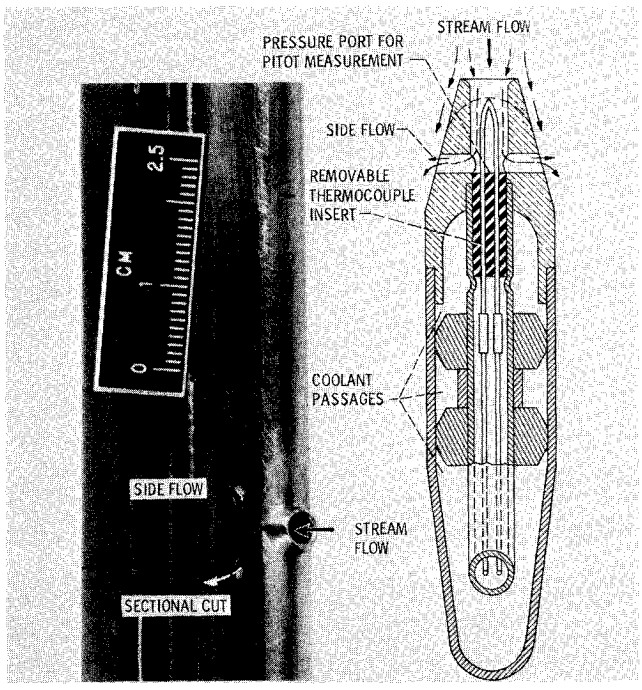

Fig. 6 Instrumentation rake-detail.

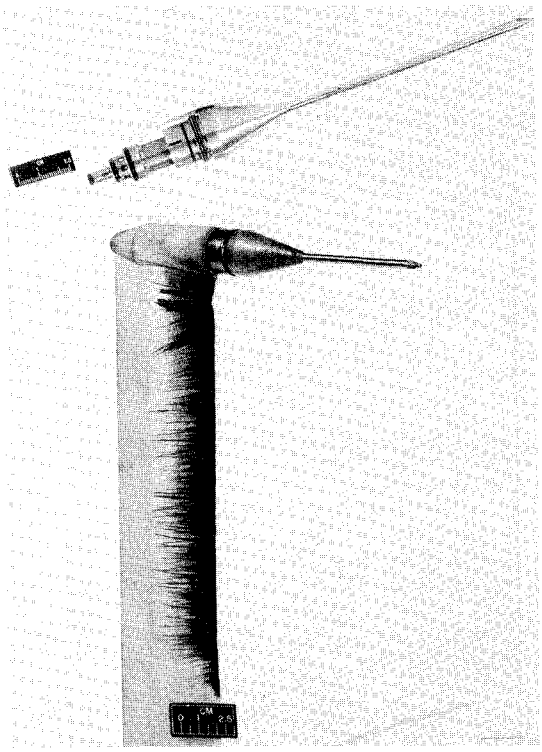

Fig. 7 Stream Pitot probe, static probe (inset), and support strut.

The traversing and interchangeable Pitot and static probe heads shown in Fig. 7 were built according to the design of high enthalpy instrumentation described in Ref. 7. The static pressure port was 21.5 probe diameters downstream of the probe tip. The strut was flamespray coated with zirconium oxide to provide additional thermal protection. At inlet stream conditions, the sharp leading edge of the strut melted back to an approximate 0.060-in. (0.154-cm) radius during the first run and the copper Pitot probe tip blunted to a 0.005-in. (0.012 cm) radius. No additional melt back occurred in subsequent runs at inlet stream conditions. At the higher temperatures at the combustor exit, however, probe damage or failure was frequent. All probe and rake structures were cooled with high-pressure water.

Combustor Inlet Conditions

Combustor inlet conditions were measured at the exit of the contoured nozzle and were assumed to be unchanged after the combustor hardware was installed. Subsequent measurement of wall static pressure in the combustor verified the validity of this assumption. Nozzle exit static pressure was measured slightly upstream of the exit plane and was extrapolated to an exit value. Pitot pressure and stream total temperature were measured 3–5 in. (7.6–12.7 cm) downstream of the nozzle exit plane in the region of parallel flow and were assumed to be constant for this distance.

The exit profiles are plotted in Fig. 8. Pitot pressure as measured by the traversing probe (Fig. 7) and as measured by a fixed multipoint rake are compared in the figure. Rake measurements were consistently lower than those with the probe, but the probe Pitot measurements are considered to be more valid. The fixed rake had a large shock detachment distance associated with the blunt leading edge so that cross flow could have occurred in the subsonic flow region along the leading edge. More logically, however, the pressure difference is believed to be related to the flow and pressure conditions which exist near the pressure port in this type of probe design. As shown in Fig. 6, the pressure port is located in a subsonic flow region behind the leading edge orifice and measures the pressure of the flow system indicated in the figure. The gas flow through the probe is driven by the difference between shock recovery pressure at the probe entrance and the static pressure at the flow vents located on the side of the rake wedge. The pressure port, thus, probably measures a pressure somwhere between these limits and records a pressure lower than a true Pitot pressure. The disparity between the probe and rake measurements was not fully investigated and is only hypothesized. The flow Mach number was calculated from the Pitot pressures plotted in Fig. 8a assuming a stream static pressure equal to the extrapolated nozzle exit wall static pressure of 8.3 psia (5.7×10^4 N/m^2). Gamma was assumed equal to 1.27 which is the value computed according to Ref. 8 for a kinetic nozzle expansion. Close agreement with the nozzle design Mach number of 2.8 as well as the flat flow profile of the combustor inlet-stream are apparent from the figure.

Combustor inlet total temperature was measured directly with the fixed multipoint rake with radiation cooled thermocouples. The measured temperature profile of the stream, corrected for radiation loss, is plotted in Fig. 8c as a function of stream diameter. Duplicate runs reproduced indicated gas temperatures, uncorrected for radiation, within ±4%. This included the reproducibility of the propellant control system and combustion process as well as the sensitivity of the measurement to the installation of the individual thermocouple in the rake structure. The accuracy of the temperatures reported is estimated to be ±5%. All measured temperatures were corrected for radiation loss. The correction was approximately 100°–185° R (54°–102° K) for the data reported for an assumed temperature dependent emissivity of 0.163–0.211. The 4450° R (2470° K) temperature level indicated for the bulk of the flow stream is in good agreement with the temperature of 4530° R (2520° K) estimated from the theoretical reaction temperature corrected to the measured rocket C^* efficiency but neglecting the heat loss to the nozzle coolant.

The measured combustor inlet conditions are summarized in Table 1 and compared to the conditions theoretically attainable with a hydrazine-nitrogen tetroxide gas generator. Combustor inlet conditions for the assumed Mach 8 flight condition are also shown in the table for comparison. It is apparent that reasonably good simulation of combustor inlet conditions for the assumed flight condition was obtained with the gas generator although the flow profiles of Mach number and temperature as measured at the combustor inlet were

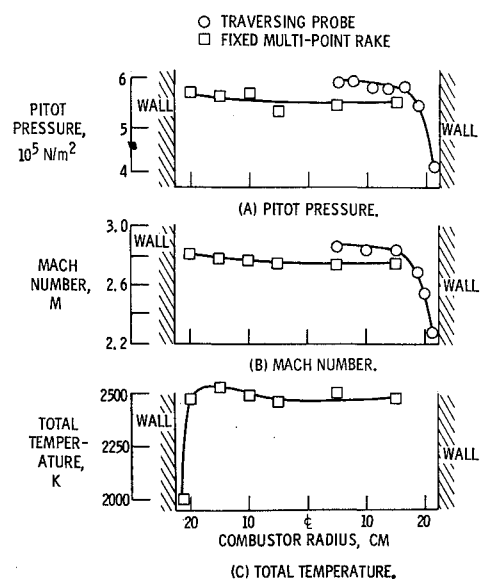

Fig. 8 Measured combustor inlet profiles.

Table 1 Comparison of Combustor inlet conditions for theory, flight, and test.

	N_2H_4–N_2O_4		Mach 8 flight, 35 km
	Kinetic expansion	Measured	
T total, °K	2680	2470	2790
T static, °K	1375	1195	1237
P total, 10^5 N/m^2	20.7	20.7	19.8
P static, 10^5 N/m^2	0.59	0.57	0.59
γ	1.268	1.26	···
Mach No.	2.87	2.87	2.87

probably flatter than would be delivered by the inlet of an actual flight vehicle. Gas samples of the combustor inlet flow stream were collected in stainless steel sample bottles for subsesequent analysis of the dry gas for nitrogen, oxygen, and nitric oxide. Nitrogen dioxide was determined by absorption photometry of the wet sample. The water content of the samples was not measured but was calculated from the oxygen atom difference between that delivered in the propellant and that measured as free oxygen and nitrogen oxides in the bottle sample. Data were limited since some samples were discarded because liquid N_2O_4 impinged on the sample ports during the oxidant lead of the start sequence and was carried into the sample bottles. These samples consequently contained a nitrogen-oxygen imbalance and were rejected.

The results of the analyses indicated a uniform gas composition across the plane of the combustor inlet having an atom composition consistent with the gas generator O/F. Only trace quantities of NO were present in the dry gas. Nitric oxide was undoubtedly a significant component of the inlet gas mixture but was measured as total NO_2 in the analytical scheme. The measured gas composition is compared in Table 2 with that calculated for a kinetic nozzle expansion according to Ref. 8. The average of six samples analyses, uncorrected for water content, is shown and reports the total NO_2 found in the sample bottle. It therefore includes both unreacted propellant NO_2 and nitric oxide which had bottle-oxidized to NO_2.

The combustor inlet gases contained a high concentration of water and the gas analysis had to be adjusted to include this water. The resulting composition is shown in the last column of Table 2 and approximates the probable composition of the combustor inlet gas stream. In calculating this composition, however, it was assumed that all of the NO_2 found in the bottle sample originated in the gas stream as nitric oxide. This assumption is probably only partly correct. Furthermore, the bottle analyses may be accurate to only 20% because of uncertainties in analytical and sampling techniques. The actual gas composition may, therefore, deviate from that indicated by the analysis but the reported values are consistent with the measured C^* efficiency of 97 to 98%. Sampling and analytical procedures favored overestimating the NO content of the sample so that the actual gas composition is believed to have had a nitric oxide composition lower than that indicated in Table 2.

Table 2 Theoretical and Analytical inlet gas composition

Mole fraction	Theoretical composition[8]	Bottle analysis	Bottle analysis including calculated water content
N^2	0.398	0.57	0.30
O_2	0.210	0.13	0.15
H_2O	0.387	···	0.39
NO	···	···	0.16
NO_2	···	0.30	···

Supersonic Combustor Tests

Basic Test Procedure

There was no precedent for testing a supersonic burning combustor of either an equivalent size or geometry at the conditions specified for this experimental program. Consequently, a rather cautious and incremental approach to the attainment of the test goals was planned. The combustor was designed to operate with a full set of sixteen hydrogen injector struts as well as hydrogen injection from the wall at a single axial station. This full configuration was approached in a step-wise manner in order to obtain the maximum information with a minimum risk to the test hardware. Combustor wall heat-transfer rates were first obtained from tests with an empty duct and were followed by testing injector struts in the increasing numbers of 1, 4, 8, and 16. Hydrogen injection rate was similarly increased progressively. For any test, minimum hydrogen flow rates were governed by the injector cooling requirements determined experimentally. The maximum hydrogen flow rate for an equivalence ratio of 1.0 was 3.2 pps (1.45 kg/sec).

Combustor Wall Heat Transfer

The inner wall of the cylindrical combustor section was $\frac{3}{16}$-in. thick Nickel 200 and was instrumented at selected locations (Fig. 5) to measure gas-side and coolant-side wall temperatures. With no burning, the wall heat-transfer rate was approximately 0.8 Btu/sec-in.^{2} (1.3×10^6 w/m^2) and gas-side heat-transfer coefficients ranged from 200–240 $\times 10^{-6}$ Btu/in.^{2}sec-°F (590–700 w/m^2-°K). Limited data with combustion indicated no major increase in wall heat transfer in the cylindrical section, but pressure measurements detected little, if any, combustion in this region. Wall heat transfer in the expansion section was not determined.

Hydrogen Injector Cooling

The basic hydrogen injector strut design incorporated a simple baffle plate at the hydrogen inlet to deflect the high velocity stream toward the leading edge of the strut. This system was proposed to force-cool the high-heat flux leading edge region of the injector. It became evident very early in the test program, however, that leading edge cooling was inadequate at the design hydrogen flow rates. Measurement of the leading edge temperature near the injector tip indicated dangerously high temperatures were reached in very short periods of time. Leading edge surface temperatures near 2600°R (1445° K) were recorded after only 14 sec of operation with a strut hydrogen flow rate of 0.25 pps which was 25% greater than the design flow rate. After 15 sec total operation, some injector damage occurred. This is illustrated in Fig. 9. In most cases, the leading edge melted and the injector split open near the strut tip. Lower hydrogen flow rates accentuated the problem.

A modification to the basic injector design was tested. The

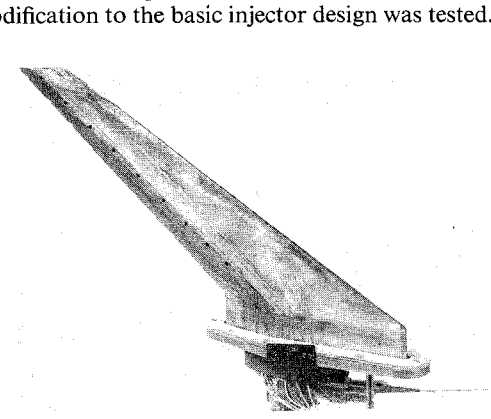

Fig. 9 Heat damaged hydrogen injector strut.

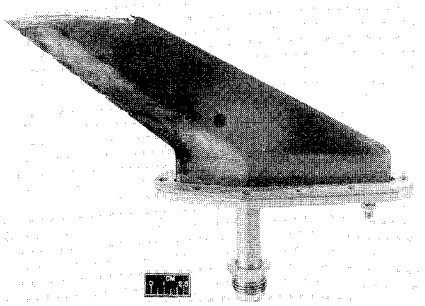

Fig. 10 Cooled leading edge hydrogen injector strut.

injector leading edge was replaced with a nickel tube of equal radius which was brazed into the structure. A separate high-pressure hydrogen supply cooled the tube and vented to the stream at the end of the injector. Coolant tube flow rates were a few percent of the main hydrogen flow to the injector. Although no injector surface temperatures were measured with this configuration, inspection indicated no leading edge damage even with injection flow rates 25% lower than required for stoichiometric burning. Even further flow reduction is believed possible without causing injector leading edge overheating. However, the vented hydrogen burned along the strut closure plate, and erosion was noted after several tests; such damage is shown in Fig. 10. Inspection of the metal flow patterns along the closure plate indicated that the vented hydrogen from the leading edge tube was shock ignited when it reached the region of the normal strut injection port in the closure plate. Subsequent design will either return the flow to the strut interior or will vent the hydrogen at the trailing edge.

Hydrogen Distribution

The gas stream was sampled at several points across the combustor exit, and the analyses were used to compute the local hydrogen equivalence ratio. The results are summarized in Fig. 11 as a function of combustor radius for samples taken only in the wake of long, first row injector struts. Also indicated on the figure are the radial locations of the individual injector ports.

Limited data with hydrogen injected only from the wall injection ring indicated that the hydrogen penetrated and spread only a short distance into the stream and remained close to the wall. Measured equivalence ratios reached 2.2 for hydrogen injection rates of 0.8 lb/sec (0.36 kg/sec). Concentration measurements at points further from the wall were not made, but it is apparent that the hydrogen concentration must rapidly fall to zero a short distance from the wall.

The lower curve of the figure describes most of the data obtained and includes data of several injector configurations ranging from only a single long strut to a complete complement of 16 struts. For these data hydrogen flow rates ranged from 0.15–0.25 lb/sec (0.07 to 0.11 kg/sec) per long injector strut. For comparison, the hydrogen flow rate would approach 0.2 lb/sec (0.091 kg/sec) per strut for stoichiometric operation with a full configuration of 16 injector struts. For all configurations represented by the curve, peak equivalence ratios only slightly greater than stoichiometric were measured and the curve was rather flat. Wall injection rates ranged from 0.2–0.4 lb/sec (0.09–0.18 kg/sec). To show the effect of an increased hydrogen injector flow rate on the hydrogen distribution, one test was made with an injector configuration of only 4 long struts. The effect of the increased hydrogen flow rate is markedly shown by the upper curve. Fuel rich mixtures were measured over almost the entire survey.

Equivalence ratio was computed from a mass spectrometer analysis of the dry sample for hydrogen, nitrogen, and oxygen. The combustor inlet composition was assumed to be the theoretical composition of Table 2 and all of the oxygen depletion was assumed to form water. The values of the equivalence ratios reported; therefore, are only approximate and may be in error by as much as 10–15%. The general levels and pattern of the hydrogen distribution, however, are believed to be valid and realistic within such limits.

Combustor Test Results

Combustor data were obtained with a full complement of 16 hydrogen injector struts, 8 in each of the two rows, and the stepped-wall injection ring. Hydrogen flow was staged between the three axial injection stations. Flow rates were 2.0 and 0.8 lb/sec (0.9 and 0.4 kg/sec) in rows 1 and 2, respectively, and 0.2 lb/sec (0.09 kg/sec) was injected from the wall. The over all combustor equivalence ratio was 0.94.

The measured stream static and Pitot pressures and the calculated Mach number profile are plotted in Fig. 12 as a

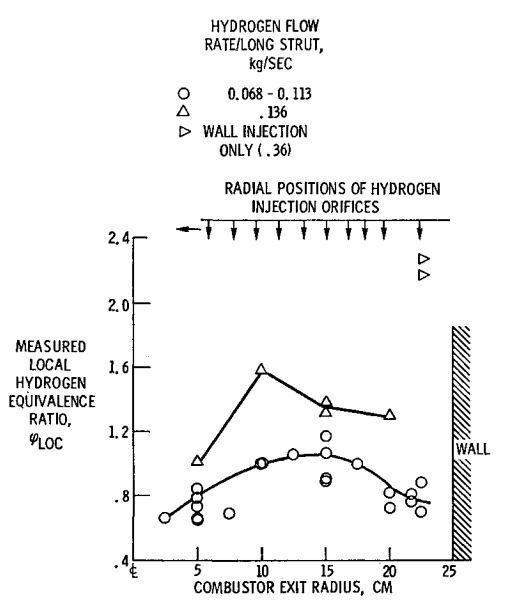

Fig. 11 Local hydrogen equivalence ratio in the wake of a long injector strut.

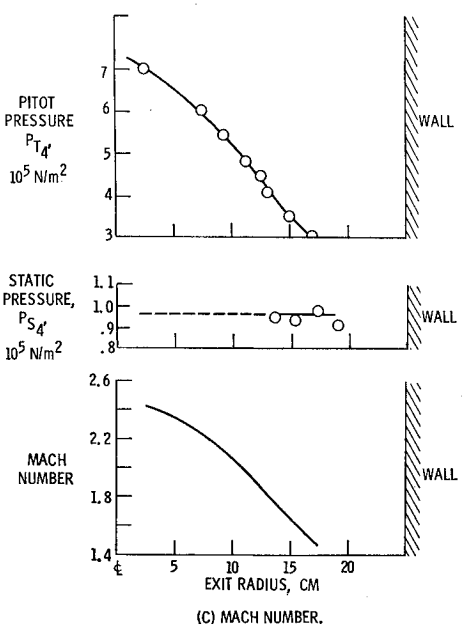

Fig. 12 Combustor exit flow profiles.

function of the combustor exit radius. The data reported were obtained at a plane approximately 6 in. (15.2 cm) downstream of the combustor exit. The instrument collar had a larger diameter than the combustor exit so the flow stream experienced a sudden expansion at the combustor exit plane. The generated expansion fan propagated downstream and intersected the probe traversal line at a radius of about 7 in. (17.7 cm). At greater radii, the measured static pressures could not be corrected for the effects of the expansion since the Mach number distribution upstream of the corner was not known. Data are reported, therefore, only to stream radii less than 7 in.

Figure 12 shows the Pitot pressures ranged from 40–102 psia (2.7 to 7.0 $\times$ 10^5 N/m^2) over the stream radius surveyed. Stream static pressures were measured only over a 5 in (12.7 cm) traverse and indicated a static pressure level for 14 psia (9.6 $\times$ 10^4 N/m^2) as shown in the figure. The probe failed before more data could be obtained.

The Mach number profile plotted in Fig. 12c was calculated from the measured Pitot pressure and assumed the stream static pressure to be 14 psia (9.6 $\times$ 10^4 N/m^2) over the stream cross section. Calculated Mach numbers ranged from 2.4–1.5 with the higher values occurring near the stream center line where prior data had indicated low fuel concentration. The Mach number was calculated from the Rayleigh Pitot relation and assumed a value for gamma of 1.22. The sensitivity of Mach number to the value of gamma, however, is low so the Mach numbers calculated are probably less in error from the gamma inaccuracy than from inaccuracies in the measurement of stream pressures.

Combustor wall static pressures were measured along two axial positions which extended the length of the combustor and which were separated by a radial arc of approximately 34° (Fig. 5). Therefore, a flow disturbance or shock wave originating from a point such as the leading edge of an injector would be detected at a different axial position in each row of pressure instrumentation depending on the relative location of the source of the disturbance and the angle of propagation. Except for such instances, the wall static pressures measured by the two different rows of instrumentation agreed within the experimental error.

Combustor wall static pressures are plotted in Fig. 13 as a function of combustor length for three different test configurations. The pressure distribution for the empty duct is plotted to indicate the base line pressure distribution for the combustor inlet flow conditions. The pressures reported are normalized with the combustor inlet pressure, P_{T2}, and are reported as the pressure ratio p_s/P_{T2}. Base line pressure ratios ranged from 0.028–0.018 from combustor inlet to exit, respectively. The effect of the oblique shock system which originated from the first row injectors is apparent in the data shown for 8 injectors with no hydrogen flow. The pressure peaks indicated are local, shock-system conditions and probably are not representative of the average circumferential pressure level.

The static pressure rise which resulted from combustion at an equivalence ratio of 0.94 is shown by the upper curve of the figure. The peak pressure ratio of 0.10 occurred 30 in. (76.2 cm) from the combustor inlet and about 4 in. (10.1 cm) into the 2° combustor expansion cone. The peak pressure corresponded to a static pressure about 3.6 times as great as the combustor inlet pressure. The shape of the combustor pressure profile was similar to data reported for smaller scale combustors which utilized wall injection for hydrogen. Data were also obtained with incomplete injector configurations. These data are not shown, but the pressure levels measured were correspondingly lower. As is evident from Fig. 12, no choking of either aerodynamic or thermal origin occurs in the duct, and the flow remains supersonic. It should especially be noted that even though the maximum local geometric blockage is 4.75%, the pressure rise due to the strut blockage is negligible. The pressure rise due to second row blockage effects was not determined but could be greater than noted for the first row injectors. This would be especially true if combustion of the first row hydrogen results in boundary layer separation in the region of the second row injectors.

Analysis

By the use of a one-dimensional momentum continuity balance across the combustor an attempt was made to estimate the combustion efficiency of the supersonic combustor when operated at an equivalence ratio of 0.94. A real gas computer program[9] was modified to include an additional species, non reacting hydrogen, with the same thermal properties as hydrogen. Since no products were specified for this species, it was carried through the equilibrium gas program as an inert. Combustion efficiency was defined as the ratio of reacting hydrogen to total hydrogen. The exit flow conditions were computed from the measured inlet momentum parameters, a calculated value for combustor drag (this included combustor skin friction and strut drag), the average fuel momentum, and the measured pressure integral acting on the conical portion of the combustor. The exit flow conditions were calculated as a function of combustor area ratio with the percentage of unburned fuel (inert hydrogen) as a parameter. The results of these calculations are shown in Fig. 14. Stream

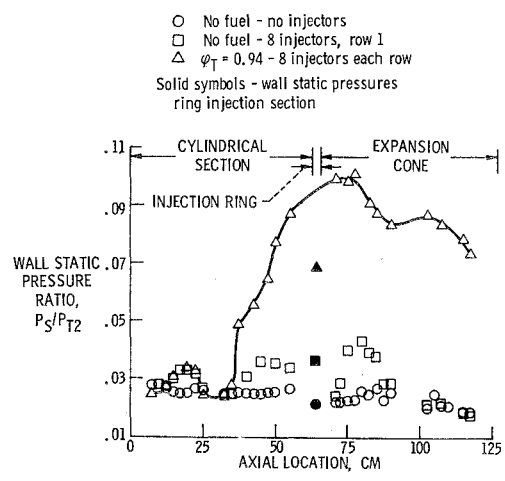

Fig. 13 Combustor wall static pressure distribution.

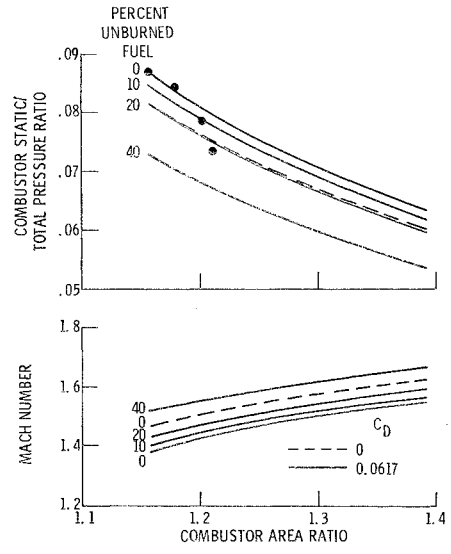

Fig. 14 The dependence of combustor pressure ratio and Mach number on combustor area ratio and combination efficiency.

static pressure ratio and Mach number are plotted against combustor area ratio. Note that the calculation did not include chemical kinetics so that each computation assumed a partial equilibrium between combustion products and inert hydrogen. The data points in the figure are the wall static pressure measurements taken from Fig. 13. The dashed curve is the plot for a combustor drag coefficient, C_D, equal to zero and complete combustion. The solid curves are calculated for a $C_D = 0.0617$ based on combustor exit area and velocity. Note that large changes in percentage of unburned fuel correspond to rather small changes in wall static pressure or Mach number, so that calculated combustion performance will be quite sensitive to measurement errors or circumferential nonuniformities. Furthermore, total pressure losses due to injector drag cannot be differentiated from incomplete combustion.

The strut drag was estimated for the first row of struts only and included the wave drag separated into forebody and aftbody components, bluntness drag of the leading edges corrected for sweepback, and skin friction drag. Base drag was negligible. The contribution of skin-friction drag for the struts and combustor wall was small compared to the strut wave drag. The drag contribution of the second row of struts could not be estimated because of the unknown flowfield upstream of the second row. Part of the wave drag for both injector rows would be offset to some extent by combustion generated pressure waves acting in the thrust direction on the rearward facing surfaces of the struts, but these forces could not be estimated in the absence of pressure measurements on the rear strut surfaces.

It is believed that any conclusions based on matching the measured wall static pressures with the calculated results would not be warranted because of both the uncertainties of the injector drag estimates and the highly non-one dimensional nature of the flow as evidenced by the wave reflections seen in the pressure profiles of Fig. 13. Since exit plane measurement of Pitot and static pressure were only partially determined along one radius and distribution of drag cannot be determined, it also did not appear warranted to attempt a more sophisticated stream tube momentum balance.

Future testing with combustors of this type should consider separate measurements of combustor thrust and drag in order to determine combustor performance.

Conclusions

The combustor tested in this program had an inlet diameter of 18 in. and used sixteen swept injector struts which penetrated the flow stream up to 78% of the combustor radius. Combustion to equivalence ratios near stoichiometric was supersonic and no choking occurred. Secondly, a new type of combustor test facility which used a rocket as a hot gas generator was demonstrated. Supersonic combustor inlet conditions simulating altitude flight at Mach 8 were closely simulated with the exhaust of the gas generator which burned storable propellants to generate vitiated high enthalpy air. For these tests one basic combustor geometry was designed after consideration of gas dynamics, chemical kinetics, and penetration and mixing criteria. This combustor design was not optimized and the test results indicate required changes for future steady-state combustor testing. Improved injector cooling is necessary, especially if hot hydrogen is to be considered for future application. Improved penetration of the hydrogen injected from the wall is also desirable to avoid over-rich regions along the combustor wall. Also, it will be necessary in future tests to measure the combustor thrust and drag in order to determine the combustor performance or combustor efficiency since profiles of stream properties measured by conventional instrumentation are too insensitive or insufficiently detailed to determine combustor performance.

References

[1] Schetz, J. A. and Billing, F. S., "Penetration of Gaseous Jets Injected into a Supersonic Srteam," *Journal of Spacecraft and Rockets*, Vol. 3, No. 11, Nov. 1966, pp. 1658–1664.

[2] Metzler, A. J. and Lezberg, E. A., "A Hot Gas Generator for Large Scale Supersonic Combustor Testing," AIAA Paper 68–647, New York, 1968.

[3] Erickson, W. D. and Klich, G. F., "Analytical Chemical Kinetic Study of the Effect of Carbon Dioxide and Water Vapor on Hydrogen-Air Constant Pressure Combustion," TN D-5768, 1970, NASA.

[4] Wanhainen, J. P. and Vincent, D. W., "Stability and Performance Characteristics of Several Hydrazine and Nitrogen Tetroxide Hot Gas Generators for Large Scale Supersonic Combustor Testing," TM X-1845, 1969, NASA.

[5] Sauer, R., "General Characteristics of the Flow Through Nozzles at Near-Critical Speeds," TM 1147, 1947, NACA.

[6] Reshotko, E. and Tucker, M., "Approximate Calculation of the Compressible Turbulent Boundary Layer With Heat Transfer and Arbitrary Pressure Gradient," TN 4154, 1957, NACA.

[7] Parobeck, D. M., "Performance of Free Stream Flow Instrumentation for 9-inch Contoured Nozzle Test in the RTD 4-Megawatt Electro Gasdynamic Facility," AFFDL-TR-65-179, DDC AD-476608L, Dec. 1965, Air Force Flight Dynamics Lab., Wright-Patterson Air Force Base Ohio.

[8] Moretti, L., "A New Technique for the Numerical Analysis of Non-Equilibrium Flows," TR-412, DDC AD-466922. March 1964, General Applied Science Labs. Inc., Westbury, N. Y.

[9] Franciscus. L. C. and Healy, J. A., "Computer Program for Determining Effects of Chemical Kinetics on Exhaust-Nozzle Performance," TN D-4144, 1967, NASA.